
Article:
Bínová, Eva, Bína, David, Ashford, David A et al. (2 more authors) (2017) Trehalose During Two Stress Responses in Acanthamoeba:Differentiation Between Encystation and Pseudocyst Formation. Protist. pp. 649-662. ISSN 1434-4610

https://doi.org/10.1016/j.protis.2017.09.001

Title: Trehalose During Two Stress Responses in *Acanthamoeba*: Differentiation Between Encystation and Pseudocyst Formation<!–<RunningTitle>Trehalose in *Acanthamoeba*</RunningTitle>–>

Authors: Eva Bínová, David Bína, David A. Ashford, Jane Thomas-Oates, Eva Nohýnková

PII: S1434-4610(17)30077-9
DOI: http://dx.doi.org/10.1016/j.protis.2017.09.001
Reference: PROTIS 25592

To appear in:

Received date: 12-5-2017
Accepted date: 7-9-2017

Please cite this article as: Bínová, Eva, Bína, David, Ashford, David A., Thomas-Oates, Jane, Nohýnková, Eva, Trehalose During Two Stress Responses in Acanthamoeba: Differentiation Between Encystation and Pseudocyst Formation.Protist http://dx.doi.org/10.1016/j.protis.2017.09.001

ORIGINAL PAPER

Trehalose During Two Stress Responses in *Acanthamoeba*: Differentiation Between Encystation and Pseudocyst Formation

Running title: Trehalose in *Acanthamoeba*

Eva Bínová[a], David Bína[b], David A. Ashford[c,d], Jane Thomas-Oates[c,e], and Eva Nohýnková[a,1]

[a]Institute of Immunology and Microbiology, First Faculty of Medicine, Charles University and General Faculty Hospital, 128 00 Prague, Czech Republic

[b]Biology Centre of the Czech Academy of Sciences and Faculty of Science, University of South Bohemia, 370 05 Ceske Budejovice, Czech Republic

[c]Centre of Excellence in Mass Spectrometry, University of York, Heslington, York, YO10 5DD, UK

[d]Technology Facility (Proteomics & Analytical Biochemistry Laboratory), Department of Biology, University of York, Heslington, York, YO10 5DD, UK

[e]Department of Chemistry, University of York, Heslington, York, YO10 5DD, UK

Submitted May 12, 2017; Accepted September 9, 2017

Monitoring Editor: C. Graham Clark

[1]Corresponding author; fax +420 224 968 525
e-mail enohy@lf1.cuni.cz (E. Nohýnková).

The non-reducing disaccharide trehalose can serve as a protectant against a range of environmental stressors, such as heat, cold, or dehydration, in both prokaryotes and eukaryotes, with the exception of vertebrates. Here, we analyzed trehalose metabolism in the facultatively parasitic organism *Acanthamoeba castellanii*, known to respond to unfavorable external conditions by forming two resistant stages: a cyst, produced in the case of chronic stress, and a pseudocyst, formed in reaction to acute stress. The possible role of trehalose in the resistant stages was investigated using a combination of bioinformatic, molecular biological and biochemical approaches. Genes for enzymes from a widespread trehalose-6-synthase-trehalose-6-phosphate phosphatase (TPS-TPP) pathway and a prokaryotic trehalose synthase (TreS) pathway were identified. The expression patterns of the genes during encystation and pseudocyst formation were analyzed and correlated with the time course of cellular trehalose content determined mass spectrometrically. The data clearly demonstrate fundamental differences between encystation and pseudocyst formation at the level of cellular metabolism.

Keywords: Trehalose; *Acanthamoeba*; cyst; pseudocyst; mass spectrometry; phylogeny.

Introduction

The genus *Acanthamoeba* (Amoebozoa) represents free-living amoebae found in disparate ecosystems all over the world. Acanthamoebae are considered the most widespread protists in nature. Moreover, under specific conditions, acanthamoebae are able to infect humans and cause rare but serious diseases, including so-called granulomatous amoebic encephalitis, a

uniformly fatal infection of the central nervous system of an immunocompromised individual, and amoebic keratitis, a vision-threatening infection of the eye (Cabral and Cabral 2003; Schuster and Visvesvara 2004). Thus, it is evident that during their lives, acanthamoebae face fundamentally different environmental stressors. The life cycle of *Acanthamoeba* consists of two mononuclear stages: an active amoeba (a trophozoite) and a dormant cyst. *Acanthamoeba* cysts are formed upon exposure of trophozoites to long-lasting unfavorable environmental conditions, such as drought or starvation (Neff et al. 1964). Cysts are also formed in brain or cornea tissues during chronic infection. According to in vitro experiments, encystation, i.e., transformation of a trophozoite into a cyst, takes 16-24 hours (Köhsler et al. 2008; Lloyd et al. 2001). In the course of this process, the cell volume decreases, and a double-layered wall assembles on the cell surface. Cellulose is the main component of the inner cyst wall layer (known as the endocyst), whereas the outer layer (the exocyst) is mostly proteinaceous (Bowers and Korn 1969; Weisman 1976). As a cyst, *Acanthamoeba* cells can remain viable for years (Aksozek et al. 2002; Mazur et al. 1995). Recently, Kliescikova et al. (2011a) found that under acute stress (induced in vitro by exposure of cells to organic solvents), trophozoites rapidly differentiate into pseudocysts, another stage enabling acanthamoebae to survive life-threatening conditions. Pseudocyst formation was also observed in acanthamoebae exposed to contact lens solutions containing propylene glycol (Kliescikova et al. 2011b) and in marine parasitic amoeba *Neoparamoeba perurans* when subjected to fresh water (Lima et al. 2017). In contrast to cysts, *Acanthamoeba* pseudocysts are formed within two hours, their surface is covered with a single-layered fibrillar mannose/glucose coat, the cyst-specific protein CSP21 is not expressed, and their resistance to temperature, pH or desiccation is limited (Kliescikova et al. 2011a). Thus, *Acanthamoeba* can modify a cellular stress response according to external stimuli. A recent analysis of the genome of *A. castellanii* revealed many proteins that were putatively involved in the modulation of the cellular response to external cues. This analysis

included a large number of protein kinases of different kinase families (Clarke et al. 2013). However, other mechanisms involved in the defense of the internal environment of the *Acanthamoeba* cell during adaptation to stress remain poorly understood, and the available experimental data are limited to the characterization of ultrastructural changes, chemical composition of the envelope and resistance parameters of the resting stages (Bowers and Korn 1969; Kliescikova et al. 2011a; Weisman 1976).

In many eukaryotes, stress resistance is accompanied by the synthesis of protective compounds to alleviate the effects of anhydrobiosis, freezing, and osmotic pressure on macromolecular assemblies such as membranes. This role is often played by carbohydrates, trehalose or the sugar alcohol mannitol, as described previously (Lourenço et al. 2016). In the genome of *A. castellanii*, genes coding for several enzymes of biosynthetic pathways for mannitol and trehalose have been reported, and protective roles for these compounds have been suggested (Anderson et al. 2005; Watkins and Gray 2008). However, despite previous identification of putative genes involved in the synthesis of mannitol, we recently found (Binova et al. 2012) that mannitol is not present in either stage of the *Acanthamoeba* life cycle. Therefore, we aimed to further investigate the presence and synthesis of trehalose during the formation of the stress-resistant stages of acanthamoebae. Moreover, a recent study by Clarke et al. (2013) of the genome of *A. castellanii* enabled our investigation of the molecular mechanisms of trehalose synthesis in detail.

Trehalose is a non-reducing disaccharide formed from two glucose units linked together in an α, α -1, 1-glycosidic linkage, which makes it a very stable molecule. Trehalose occurs in a wide variety of organisms, including archaea, bacteria, protists, plants and arthropods (Elbein et al. 2003). There are at least five different pathways for its synthesis described in bacteria (Avonce et al. 2006, Paul et al. 2008). The most widely distributed and best-known pathway involves two catalytic steps. In the first step, trehalose-6-phosphate

synthase (TPS) transfers glucose from UDP-glucose to glucose-6-phosphate to form trehalose-6-phosphate. Subsequently, trehalose-6-phosphate is dephosphorylated via trehalose-6-phosphate phosphatase (TPP) to produce trehalose (Elbein et al. 2003; Iordachescu and Imai 2008). This is the only pathway that was also conclusively demonstrated in eukaryotes (Roth and Sussman 1966). Of the four remaining pathways, three are found in both bacteria and archaea (Avonce et al. 2006). The trehalose-synthase pathway, whereby trehalose is formed from maltose in a single transglycosylation reaction via trehalose synthase (TreS), is considered unique to bacteria (Avonce et al. 2006; Paul et al. 2008).

In this study, we searched the *Acanthamoeba* genome for putative enzymes involved in trehalose synthesis pathways. The recovered sequences were analyzed and placed into the phylogenetic context. Using qPCR, we followed a time course of expression of mRNA for these proteins during encystation and pseudocyst formation and determined correlations between the mRNA expression patterns of the enzymes and concentrations of cellular carbohydrate pools. Based on the results, we propose the presence of two functional pathways of trehalose synthesis in *Acanthamoeba*. Moreover, our results clearly support the view that encystation and pseudocyst formation, the two stress responses of *Acanthamoeba*, represent fundamentally different processes.

Results

Phylogenetic Analyses

As the first step, we searched the genome of *A. castellanii* for the presence of genes coding for enzymes known to participate in trehalose synthesis in other organisms (Avonce et al. 2006). We identified four putative genes from two trehalose synthesis pathways, namely, a single gene for TreS and three variants of a fusion gene for the TPS-TPP fusion protein. No

single-domain TPS or TPP enzymes were found. Next, we analyzed the phylogenetic context of the genes.

TreS in *Acanthamoeba*

The presence of a gene for TreS in the genome of *A. castellanii* has already been suggested by Clarke et al. (2013). Our search supported this finding. The BLAST search based on the *A. castellanii* sequence also showed the presence of putative TreS sequences among other species of free-living Amoebozoa. TreS is a member of oligo-1, 6-glucosidase subfamily of the GH13 family of glycoside hydrolases (Kuriki and Imanaka 1999). To determine the identity of the putative amoebic TreS unambiguously, we assembled a dataset covering the whole range of diversity of the GH13 hydrolases and subjected it to a phylogenetic analysis. As shown (Fig. 1), the sequences retrieved from representatives of Amoebozoa clearly belonged to the TreS subfamily of GH13 hydrolases forming a monophyletic group. All methods of phylogeny reconstruction placed the Amoebozoa sequences in the basal position with respect to the bulk of prokaryotic proteins. Interestingly, all Amoebozoa TreS sequences lacked the C-terminal domain. This domain with a probable kinase activity is fused to TreS in many groups of bacteria, e.g., proteobacteria, cyanobacteria and chlorobi (Jarling et al. 2004). The topology of the tree (Fig. 1) suggests that the C-terminal domain represents a later addition to the TreS enzymes and that the acquisition of the TreS gene by an ancestor of the extant amoebae preceded the C-terminal fusion. The absence of the C-terminal domain is an aspect shared by the Amoebozoa and actinobacteria, of which the high-resolution structure of TreS is available (*Mycobacterium avium* and *M. smegmatis*) (Caner et al. 2013, Roy et al. 2013). Comparative analysis of the Amoebozoa TreS with the mycobacterial enzymes revealed the conservation of the catalytic residues and the domain organization of the enzyme

(Fig. 2). This finding indicates that the TreS sequence recovered from the *Acanthamoeba* genome represents an active enzyme.

TPS-TPP in *Acanthamoeba*

Because we identified only fusion genes for TPS-TPP (see above), both domains were analyzed together in the phylogenetic analysis as in Yu et al. (2010). The phylogenetic position of the TPS-TPP proteins from *A. castellanii* is shown in Figure 3. The sequence, hereafter denoted TPS-TPP 1, is placed at the base of all eukaryotic enzymes. The other two, denoted TPS-TPP 2A and 2B, are positioned at the base of the group of fungal enzymes. The tree was rooted using the prokaryotic protein sequences. In both cases, the sequences retrieved from *A. castellanii* were grouped with the TPS-TPP enzymes from other Amoebozoa species.

The genomes of many organisms contain multiple copies of the enzymes of the TPS-TPP pathway, with many of these copies likely coding for enzymatically inactive proteins serving regulatory or structural functions (Avonce 2006). Thus, the sequences of the TPS-TPP from *A. castellanii* were analyzed in more detail to assess their functionality. Sequences from *Saccharomyces cerevisiae* were chosen because this model organism contains a set of TPS-TPP pathway enzymes, including both active and inactive forms, and the course of its TPS-TPP pathway is well understood (Gancedo and Flores 2004). Furthermore, sequences of single-domain TPS and TPP proteins of which high-resolution structures are known were included in the comparison (OtsA from *Escherichia coli*, PDB: 1GZ5 for TPS and TPP from *Thermoplasma acidophilum*, PDB: 1U02). These analyses indicate complete conservation of the catalytic residues of the TPS domain of the primitive TPS-TPP 1 protein sequence but not in TPS-TPP 2A and 2B of the 'fungal' clade (Fig. 4). In contrast, in the TPP domain, TPS-TPP1 lacked several conserved catalytic residues that were present in TPS-TPP 2A and 2B (Fig. 5). Assuming that the absence of several of the conserved catalytic residues implies the

absence of the catalytic function, TPS-TPP 1 is deficient in TPP activity, whereas TPS-TPP 2A and 2B lack TPS activity. Thus, the two phylogenetically distinct types of TPS-TPP appear to be able to complement each other in providing the complete pathway of trehalose synthesis in *Acanthamoeba*.

The bioinformatic analyses suggests that *A. castellanii* possesses a functional enzymatic apparatus of two pathways for the synthesis of trehalose. To test whether these pathways actively participate in the stress defense response, we analyzed the expression patterns of the enzymes and monitored the cellular carbohydrate levels during encystation and pseudocyst formation.

Gene Expression of Enzymes for Trehalose Synthesis During *Acanthamoeba* Differentiation

To explore the expression patterns of genes for trehalose synthesis during encystation and pseudocyst formation, we performed a qRT-PCR analysis of all four trehalose synthesis genes found in the *Acanthamoeba* genome, namely, TPS-TPP 1, TPS-TPP 2A, TPS-TPP 2B and TreS.

In *Acanthamoeba* cells undergoing differentiation into pseudocysts (Fig. 6A), all these enzymes were upregulated within a maximum of 30 minutes after initiation/induction of the process and gradually decreased thereafter until the last time interval monitored in our experiments (72 hours). Nevertheless, the mRNA levels for all studied genes always exceeded the levels in the trophozoites.

In encysting cells (Fig. 6B), genes of only two of the enzymes, namely TPS-TPP 2B and TreS, showed higher expression than in the trophozoites. Maximum expression was observed 2 hours post-induction. During the next 12 to 24 hours, gene expression of both enzymes declined substantially. Within the next 48 hours, the levels of mRNAs of both

enzymes dropped below the levels determined in the trophozoites (representing the level at time zero) (Fig. 6B, time intervals from 48 to 72 hours). The expression of two other genes, namely TPS-TPP 1 and TPS-TPP 2A, was repressed during the whole process of encystation. During the first two hours, the amount of the mRNA for these enzymes was slightly lower compared to the amount at time zero (the trophozoite stage), and it continued to decrease until the end of the monitoring period (72 hours).

Regarding changes in mRNA expression of the trehalose synthesis genes, there were considerable differences between pseudocyst formation and encystation: up to 50-fold enhancement during the former compared to a maximum increase of two-fold during the latter (Fig. 6A, B).

Quantitative Changes in Carbohydrate Levels in Differentiating Acanthamoebae

Mass spectrometric quantification was used to determine the amounts of trehalose as well as those of glucose and maltose that may serve as substrates for trehalose synthesis in *Acanthamoeba* cells undergoing encystation or pseudocyst formation. The analysis first revealed that trehalose is present in all *Acanthamoeba* stages, trophozoites, mature pseudocysts and mature cysts (Fig. 7). While in the mature pseudocyst (Fig. 7A: time interval, 2 hours), the amount of trehalose was approximately 50% less than in the trophozoite. In the mature cyst (Fig. 7B: time interval, 24 hours), the level of this carbohydrate was approximately 30% higher than that in the trophozoite. During differentiation of the trophozoites to the pseudocysts, the level of trehalose showed two peaks, at 0.5 and 24 hours post-induction (Fig. 7A), that were separated by a transient decrease at approximately 2 hours (a pseudocyst maturation). During encystation, a marked increase in the trehalose levels occurred at 12 hours, and they remained elevated for up to 48 hours, followed by a decrease at 72 hours (Fig. 7B). The glucose level detected in the trophozoites (Fig. 7 A, B; time interval,

0.1 hours) markedly dropped at the beginning of both processes (Fig. 7A, B; time interval, 0.5 hours). A subsequent decrease was observed at 2 and 12 hours for pseudocyst formation and encystation, respectively. The amounts of maltose decreased 30 minutes after the induction of pseudocyst formation (Fig. 7A) and 12 hours after the induction of encystation (Fig. 7B). The levels of maltose and glucose were approximately zero in the mature pseudocysts (time intervals from 2 to 72 hours) and very low in the mature cysts (time intervals from 24 to 72 hours).

Discussion

Phylogenetic Analysis

In this paper, we present evidence that the genome of *A. castellanii* contains genes for enzymes from two different pathways for trehalose synthesis, the prokaryotic TreS and the widespread TPS-TPP-based pathways, and that according to the bioinformatics data, these pathways are functional.

The phylogenetic analysis, which determined *Acanthamoeba* TreS to be a member of the TreS subfamily that forms a monophyletic group together with other Amoebozoa on the basis of the TreS part of the tree, suggests a single gene transfer event preceding the diversification of the extant Amoebozoa members. Moreover, all methods of phylogenetic reconstruction placed Amoebozoa TreS sequences in the basal position with respect to the bulk of prokaryotic proteins. Such placement of the eukaryotic TreS might be a result of faster molecular evolution of bacteria than eukaryotes, leading to faster divergence of the bacterial sequences. This possibility implies that the eukaryotic TreS sequence might in fact represent a more primitive form of the protein.

Comparison of the *A. castellanii* TreS sequence to the bacterial enzyme showed a complete conservation of the catalytic residues. Of the conserved regions, one of particular interest is the FLRNH**DE**L**L**TLEMVT motif in the extended active loop of domain A (blue in Fig. 2). Among the GH13 hydrolases studied, we found this motif to be unique to TreS, thus offering the possibility of rapid identification of TreS in other organisms of interest. We have applied this to another important representative of facultative pathogenic amoebozoa, *Balamuthia madrillaris*. Blast search (tblastn using *A. castellanii* TreS sequence) of the two available assemblies of *B. madrillaris* genomes (strain CDC-V039, accession LFUI01000000 and strain 2046, LEOU01000000) revealed candidates for TreS enzyme in this species as well (LFUI01000178 and LEOU01000424, respectively).

While the presence of the prokaryotic TreS pathway of trehalose synthesis in Amoebozoa is somewhat surprising (Avonce et al. 2006; Paul et al. 2008), the presence of the TPS-TPP enzymes could be expected, as they were found in a wide range of organisms from archaea to higher plants, the latter possessing multiple copies of the TPS-TPP proteins. Avonce et al. (2010) divided the TPS-TPP protein sequences of the amoebozoan slime mold *Dictyostelium discoideum* into two separate groups of enzymes, one associated closely with prokaryotic fused (TPS-TPP) enzymes and the other on the basis of the fungal sequences. Our results based on the phylogenetic analysis of the three *A. castellanii* fused TPS-TPP sequences (Fig. 3), are clearly consistent with the findings of Avonce et al. (2010), and show very similar topology.

Gene Expression of Enzymes for Trehalose Synthesis in *Acanthamoeba* Stress Responses

We further show that genes for all four trehalose biosynthetic enzymes found in the *Acanthamoeba* genome are expressed during both types of stress reactions. Because the bioinformatics data indicate catalytic activity for each of the encoded enzymes, their

expression suggests that trehalose and/or its precursors are important components of stress reactions. However, we can only speculate about the functions of the enzymes and roles of the carbohydrate during a response by this protist to environmental stress. It must be kept in mind that the observed amounts of mRNAs are not necessarily an unambiguous indicator of protein levels or activity of the respective enzymes. Hence the following section aims to integrate the discussion of changes in gene expression of enzymes of trehalose synthesis and observed kinetics of carbohydrate levels.

Gene Expression of Enzymes for Trehalose Synthesis During Pseudocyst Formation

During formation of the pseudocysts, we observed the most pronounced increase in mRNA expression for all four genes within the first 30 minutes. A rapid shock reaction by *Acanthamoeba* cells has been described at this time point: the cells become rounded, detach themselves from the substrate and start to synthesize and export material for a fibrillar coat on the cell surface (Kliescikova et al. 2011a). It seems likely that in these early/immature pseudocysts, TreS predominates in the synthesis of trehalose since the increase in the amount of trehalose apparently correlates with a decrease in maltose, a substrate for trehalose synthesis in the TreS pathway (Nishimoto et al. 1995). The function of trehalose in this phase of *Acanthamoeba* differentiation is unknown. In general, trehalose may serve as an energy and carbon source, a signaling or regulation molecule, a cell wall component, or a membrane and protein protectant (Elbein et al. 2003). A significant decrease in trehalose in the maturing pseudocysts indicates the former possibilities. At the same time, a role for the enzymes of the TPS-TPP pathway remains completely unclear. Provided that all the trehalose detected at the 30-minute time point was formed by converting maltose via TreS, the TPS-TPP pathways could not be involved in trehalose synthesis; the increase in trehalose levels correspond to the decrease in maltose over the first 30 mins (Fig. 7A), consistent with the 1:1 conversion

catalyzed by TreS. On the other hand, the activities of these enzymes may yield other important molecules, such as those in plants, where trehalose-6-phosphate (T6P), the metabolic precursor of trehalose in the TPS-TPP biosynthetic pathway, is an important signaling metabolite (O´Hara et al. 2013).

Interestingly, we observed another increase in the trehalose level in the mature pseudocysts (between 2 and 24 hours). Because the concentration of maltose was approximately zero after 30 minutes of differentiation, it seems that in the mature pseudocysts, trehalose is formed particularly via the TPS-TPP pathways. Moreover, in contrast to the immature pseudocysts, the mature forms that possess a fine fibrillar coat covering the entire cell surface are, to a certain extent, resistant to heat and desiccation (Kliescikova et al. 2011a), suggesting a need for compounds that protect the inner environment of the mature pseudocyst from the deleterious effect of thermal and drought stress. However, further experiments are needed to determine whether trehalose is the protective compound.

Gene Expression of Enzymes for Trehalose Synthesis During Encystation

Unlike with pseudocyst formation, we detected upregulation of only two of the four genes of trehalose synthetic enzymes, TreS and TPS-TPP 2B, during *Acanthamoeba* encystation. As with the immature pseudocysts, the TreS pathway seemed to play a major role in trehalose synthesis in the encysting acanthamoebae since TreS was found to have the highest expression level of mRNA and since an increase in trehalose was mirrored by a decrease in maltose. However, a comparison of the levels of the two disaccharides clearly shows that maltose could not be the only substrate for trehalose synthesis. Involvement of the TPS-TPP pathway was indicated by upregulation of TPS-TPP 2B gene with a very similar trend to TreS, i.e., a gradual increase during the first two hours of encystation, followed by a sharp

decrease. This observation suggests that either TPS-TPP 2B represents a fully active enzyme capable of catalyzing both steps of the trehalose synthesis, despite the amino acid substitutions, or that TPS-TPP 2B acts as a part of a multi-component complex, either by providing the TPP activity or playing a regulatory role, similar to Tsl1 and Tps3 in *Saccharomyces* (Gancedo and Flores 2004). This finding implies that other components of a putative complex, e.g., TPS-TPP 1, which contains an active TPS domain, are already present in the cell prior to the onset of encystation.

Surprisingly, after 24 hours of encystation, the amount of trehalose gradually decreased, indicating a partial breakdown of the disaccharide within the mature cysts. The final trehalose level observed was even less than that in the trophozoites or pseudocysts but likely persisted thereafter as a store. Using ^{13}C NMR spectroscopy, Deslauriers et al. (1980) detected stable levels of trehalose in 16- and 77-day-old cysts of *A. castellanii.* However, nothing is known about why and how the level of trehalose synthesized during the process of encystation is later (after 12 hours) reduced within the cysts. Mature *Acanthamoeba* cysts are represented by highly resistant non-motile cells (thanks to a fully developed double-layered cyst wall) with a reduced total volume, dense cytoplasm due to dehydration by water expulsion, fewer organelles in comparison with trophozoites and minimal metabolic activity (Bowers and Korn 1969). The cysts are very limited in energy resources; they cannot use exogenous nutrients, and endogenous energy supplies, especially glycogen, are mostly depleted for cyst-wall synthesis or are excreted into the outer space of the encysting cell during autophagy (Khan 2009). Thus, one possibility is that trehalose hydrolysis could provide an energy or carbon source in the mature cysts. Trehalose degradation may also be necessary to stabilize the internal osmolarity of long-living *Acanthamoeba* cysts. In the *Acanthamoeba* genome, there are four enzymes (NCBI accession numbers XP_004344107.1, XP_004340178.1, XP_004335070.1, and XP_004335069.1) possessing the glycosyl

hydrolase family 65 catalytic domain (Bínová, unpublished) that can hydrolyze trehalose. This enzyme family contains the vacuolar acid trehalase (Davies and Henrisat 1995), with a widespread occurrence in fungi (Thevelein 1984). On the other hand, similarly to in the mushroom *Agaricus bisporus* (Wannet et al. 1998), trehalose may also be degraded by the phosphorylase activity of TPS-TPP 2B provided that the *Acanthamoeba* enzyme catalyzes the phosphorolysis of trehalose.

To summarize, we have detected the presence of the prokaryotic TreS pathway in a eukaryotic free-living amoeba, *A. castellanii*. Although in some bacteria TreS functions bi-directionally, from maltose to trehalose and vice versa with a preference for the catabolic, not anabolic, direction (Miah et al. 2010), our results support the traditional view of *Acanthamoeba* TreS as the enzyme producing trehalose at the expense of maltose, during both encystation and pseudocyst formation. The active apparatus for trehalose synthesis and the presence of a large amount of trehalose during encystation and pseudocyst formation point to an important role for trehalose in *Acanthamoeba* stress responses, but the exact functions of this disaccharide remain to be elucidated. We have shown that trehalose is present in all known forms of *Acanthamoeba,* i.e., the vegetative trophozoites and two stress-induced stages, pseudocysts and cysts. We have also shown quantitative changes in the amount of trehalose during encystation and pseudocyst formation. Finally, our results clearly show that encystation and pseudocyst formation represent two fundamentally different responses of acanthamoebae to stress.

Methods

Cell culture and culture conditions: Clinical isolate V1 of *Acanthamoeba* spp., T4 genotype (Kliescikova et al. 2011a, b) was grown axenically in 25, 75 or 175 cm^2 culture flasks

(Corning, USA) in PYG medium supplemented with 500 IU/mL penicillin at 37°C (Bínová et al. 2012).

Induction of encystment and pseudocyst formation: To induce encystation, *Acanthamoeba* trophozoites in the exponential phase of growth were overlaid with Neff encystation medium (NEM) (Neff et al. 1964), composed of 100 mM KCl, 8 mM $MgSO_4$ • 7 H_2O, 4 mM $CaCl_2$ • 2 H_2O, 1 mM $NaHCO_3$, and 20 mM ammediol (2-amino-2-methyl-1,3-propanediol; Sigma, USA), pH 8.8, at 37 °C. For pseudocyst induction, a protocol by Kliescikova et al. (2011a, b) was followed. Briefly, trophozoites in the exponential phase of growth were overlaid with NEM containing 1% (v/v) methanol and incubated at 37 °C. The course of encystation and pseudocyst formation was observed and evaluated by light microscopy.

RNA extraction and qRT-PCR: Total RNA was extracted at 0, 0.5, 2, 12, 24, 48, and 72 hours during encystation and pseudocyst formation using a High Pure RNA Isolation Kit (Roche) according to the manufacturer's instructions. The forming cysts (starting at 12 hours) and pseudocysts (starting at 2 hours) were homogenized using MagNA Lyser (Roche) prior to RNA extraction. Samples were subsequently treated using a TURBO DNA-free™ Kit (Ambion) to remove contaminating genomic DNA. The quality and concentration of the isolated RNA was measured using a NanoDrop spectrophotometer. cDNA synthesis was performed using a Revert Aid™ First Strand cDNA Synthesis Kit (Fermentas, EU) according to the manufacturer's instructions. One microgram of RNA was used for each reaction. For quantitative real-time PCR (qRT-PCR), 1 µL of a 10-fold dilution of cDNA solution was used in the 5-µL reaction including 2.5 µL of SYBR Green Master mix (Roche), 0.5 µL gene-specific forward and reverse primer solution (Tab. 1) designed by the Primer Quest program (http://eu.idtdna.com/Scitools/Applications/Primerquest/) and 0.5 µL pure water. qRT-PCR amplification was performed on a Light Cycler LC480 (Roche) with the following cycling

conditions: pre-denaturation (1 cycle) - 10 minutes at 95 °C; amplification (50 cycles) - 10 seconds at 95 °C, 15 seconds at 60 °C, and 15 seconds at 72 °C; melting curve (1 cycle) - 5 seconds at 95 °C and 1 minute at 65 °C; and cooling to 37 °C. As a reference gene, the gene for *Acanthamoeba* 18S rDNA was used. The experiments were done in triplicate.

Mass spectrometry: Carbohydrates were isolated from 1×10^7 cells at 0, 0.5, 2, 12, 24, 48, and 72 hours during *Acanthamoeba* encystation and pseudocyst formation (forming cysts, starting at 12 hours, and pseudocysts, starting at 2 hours, were homogenized using a bead beater prior to extraction) using the method described by Antonio et al. (2007). Carbohydrates were then quantified using external calibration HILIC ESI-qTOF-MS, based on the method described by Antonio et al. (2008). The binary LC gradient consisted of 0.1% formic acid with 5 mM ammonium acetate (solvent A) and acetonitrile containing 0.1% formic acid (solvent B) at a flow rate of 0.2 mL min^{-1}. The gradient used was as follows: hold at 90% B for 5 minutes, a linear gradient to 40% B over 24 minutes, stepping to 20% B and holding for 2 minutes, stepping to 90% B, and equilibration for 14 minutes. The data were acquired on a QSTAR pulsar *I* mass spectrometer in the negative ion mode, using the TurboIonSpray source (capillary voltage -3500 V, nebulizer gas setting 70, TurboIon gas setting 20, source temperature 200 °C, curtain gas setting 30, declustering potential (DP) -10, DP2 -10, FP -50, CAD setting 3), with acquisition over the *m/z* range 138-1000 with a 1-s acquisition time. Glc showed the weakest mass spectrometric response, with 50 pmol showing a signal:noise ratio of approximately 6:1. The mass-spectrometry analysis were done in duplicate as two separate experiments performed about six months apart. In the experiments, the differences between concentrations for respective time points were within the range of 350pmol, typically less than 15%, thus trends in the sugar concentrations were stable in two considerably different populations without necessity to perform more measurements.

Phylogenetic analyses: Multiple sequence alignment was performed with MAFFT using the E-INS-i approach with default settings (Katoh et al. 2005, 2011). Maximum likelihood analysis was performed with TreeFinder (ver. 2011, Jobb et al. 2004, Jobb 2011). Bayesian analyses were performed with MrBayes v. 3.2.2 under the WAG substitution model with a proportion of invariant sites and 4-rate gamma distribution (WAG+I+Γ_4). Neighbor joining was performed in MEGA 6 (Tamura et al. 2013) with the JTT substitution model.

Acknowledgements

This work was supported by the Grant Agency of the Czech Republic (grant number 310/09/1120); the Grant Agency of Charles University (grant number 153610); and Charles University (institutional projects Progres, number Q26/LF1, and SVV, number 260 369). D.B. acknowledges institutional support RVO: 60077344. The York Centre of Excellence in Mass Spectrometry was created thanks to a major capital investment through Science City York, supported by Yorkshire Forward with funds from the Northern Way Initiative.

References

Aksozek A, McClellan K, Howard K, Niederkorn JY, Alizadeh H (2002) Resistance of *Acanthamoeba castellanii* cysts to physical, chemical and radiological conditions. J Parasitol **88**:621–623

Anderson IJ, Watkins RF, Samuelson J, Spencer DF, Majoros WH, Gray MW, Loftus BJ (2005) Gene discovery in *Acanthamoeba castellanii* genome. Protist **156**:203-214

Antonio C, Larson T, Gilday A, Graham I, Bergstrom E, Thomas-Oates J (2007) Quantification of sugars and sugar phosphates in *Arabidopsis thaliana* tissues using porous graphitic carbon liquid chromatography-electrospray ionization mass spectrometry. J Chromatogr A **1172**:170-178

Antonio C, Larson T, Gilday A, Graham I, Bergstrom E, Thomas-Oates J (2008) Hydrophilic interaction chromatography/electrospray mass spectrometry analysis of carbohydrate-related metabolites from *Arabidopsis thaliana* leaf tissue. Rapid Commun Mass Spectrom **22**:1399-1407

Avonce N, Mendoza-Vargas A, Morett E, Iturriaga G (2006) Insights on the evolution of trehalose biosynthesis. BMC Evol Biol **6**:109

Avonce N, Wuyts J, Verschooten K, Vandesteene L, Van Dijck P (2010) The *Cytophaga hutchinsonii* ChTPSP: First characterized bifunctional TPS–TPP protein as putative ancestor of all eukaryotic trehalose biosynthesis proteins. Mol Biol Evol **27**:359–369

Binova E, Kliescikova J, Ashford DA, Thomas-Oates J, Nohynkova E (2012) Mannitol is not involved in protective reactions of *Acanthamoeba*. Mol Biochem Parasitol **184**:118-121

Bowers B, Korn ED (1969) The fine structure of *Acanthamoeba castellanii* (Neff strain) II. Encystment. J Cell Biol **41**:786–805

Cabral MF, Cabral G (2003) *Acanthamoeba* spp. as agents of disease in humans. Clin Microbiol Rev **16**:273- 307

Caner S, Nguyen N, Aguda A, Zhang R, Pan YT, Withers SG, Brayer GD (2013) The structure of the *Mycobacterium smegmatis* trehalose synthase reveals an unusual active ste configuration and acarbose-binding mode. Glycobiology **23**:1075-1083

Clarke M, Lohan AJ, Liu B, et al. (2013) Genome of *Acanthamoeba castellanii* highlights extensive lateral gene transfer and early evolution of tyrosine kinase signaling. Genome Biol **14**: R11

Davies G, Henrissat B (1995) Structures and mechanisms of glycosyl hydrolases. Structure **3**: 853-859

Deslauriers HC, Jarrell R, Byrd A, Smith ICP (1980) Observation by C-13 NMR of metabolites in differentiating amoeba – trehalose storage in encysted *Acanthamoeba castellanii*. FEBS Lett **118**:185-190

Elbein AD, Pan YT, Pastuszak I, Carroll D (2003) New insights on trehalose: a multifunctional molecule. Glycobiology **13**:17R–27R

Gancedo C, Flores CL (2004) The importance of a functional trehalose biosynthetic pathway for the life of yeasts and fungi. FEMS Yeast Res **4**:351-359

Gibson RP, Turkenburg JP, Charnock SJ, Lloyd D, Davies GJ (2002) Insights into trehalose synthesis provided by the structure of the retaining glucosyltransferase OtsA. Chem Biol **9**:1337–1346

Iordachescu M, Imai R (2008) Trehalose biosynthesis in response to abiotic stresses. J Integrative Plant Biol **50**:1223–1229

Jarling M1, Cauvet T, Grundmeier M, Kuhnert K, Pape H (2004) Isolation of mak1 from *Actinoplanes missouriensis* and evidence that Pep2 from *Streptomyces coelicolor* is a maltokinase. J Basic Microbiol **44**:360-373

Jobb G (2011) TREEFINDER version of March 2011. Munich, Germany

Jobb G, von Haeseler A, Strimmer K (2004) TREEFINDER: a powerful graphical analysis environment for molecular phylogenetics. BMC Evol Biol **4**:18

Katoh K, Standley DM (2013) MAFFT Multiple Sequence Alignment Software Version 7: Improvements in Performance and Usability. Mol Biol Evol **30**:772-780

Katoh K, Kuma K, Toh H, Miyata T (2005) MAFFT version 5: improvement in accuracy of multiple sequence alignment. Nucleic Acids Res **33**:511-518

Khan NA (2009) *Acanthamoeba*: Biology and Pathogenesis. Caister Academic Press, Norfolk UK, 2009. ISBN: 978-1-904445-43-1

Kliescikova J, Kulda J, Nohynkova E (2011a) Stress-induced pseudocyst formation--a newly identified mechanism of protection against organic solvents in acanthamoebae of the T4 genotype. Protist **162**:58-69

Kliescikova J, Kulda J, Nohynkova E (2011b) Propylene glycol and contact-lens solutions containing this diol induce pseudocyst formation in acanthamoebae. Exp Parasitol **127**:326-328

Köhsler M, Leitsch D, Fürnkranz U, Duchene M, Aspöck H, Walochnik J (2008) *Acanthamoeba* strains encyst synchronously upon prolonged axenic culture. Parasitol Res **102**:1069–1072

Kuriki T, Imanaka T (1999) The concept of the alpha-amylase family: Structural similarity and common catalytic mechanism. J Biosci Bioeng **87**:557–565

Lima PC, Taylor RS, Cook M (2017) Pseudocyst formation in the marine parasitic amoeba *Neoparamoeba perurans*: a short-term survival strategy to abrupt salinity variation. J Fish Dis **40**:1109-113

Lloyd D, Turner NA, Khunkitti W, Hann AC, Furr JR, Russell AD (2001) Encystation in *Acanthamoeba castellanii*: Development of biocide resistance. J Eukaryot Microbiol **48**:11-16

Lourenço TF, Barros PM, Saibo NJM, Abreu IA, Santos AP, António C, Pereira JS, Oliveira MM (2016) Genomics of Drought. In Edwards D, Batley J (eds) Plant Genomics and Climate Change. Springer New York, Heidelberg, Dordrecht, London, pp 85-136

Mazur T, Hadas E, Iwanicka I (1995). The duration of the cyst stage and the viability and virulence of Acanthamoeba isolates. Trop Med Parasitol **46**:106-108

Miah F, Koliwer-Brand H, Rejzek M, Field RA, Kalscheuer R, Bornemann S (2013) Flux through trehalose synthase flows from trehalose to the alpha anomer of maltose in Mycobacteria. Chem Biol **20**:487–493

Neff RJ, Ray SA, Benton WF, Wilborn M (1964) Induction of Synchronous Encystment (Differentiation) in *Acanthamoeba* spp. In Prescott DM (ed) Methods in Cell Physiology. Vol.1. Academic Press, New York, pp 55–83

Nishimoto T, Nakano M, Nakada T, Chaen H, Fukuda S, Sugimoto T, Kurimoto M, Tsujisaka Y (1995) Purification and properties of a novel enzyme, trehalose synthase, from *Pimelobacte*r sp. R48. Biosci Biotechnol Biochem **60**:640–644

O´Hara LE, Matthew JP, Wingler A (2013) How do sugars regulate plant growth and development? New insight into the role of trehalose-6-phosphate. Mol Plant **6**:261-274

Paul MJ, Primavesi LF, Jhurreea D, Zhang Y (2008) Trehalose metabolism and signaling. Annu Rev Plant Biol **59**:417–441

Rao KN, Kumaran D, Seetharaman J, Bonanno JB, Burley SK, Swaminathan S (2006) Crystal structure of trehalose-6-phosphate phosphatase–related protein: Biochemical and biological implications. Protein Sci **15**:1735–1744

Roth M, Sussman M (1966) Trehalose synthesis in the cellular slime mold *Dictyostelium discoideum.* Biochem Biophys Acta (BBA) – Enzymology and Biological Oxydation. **122**:225-231

Roy R, Usha V, Kermani A, Scott DJ, Hyde EI, Besra GS, Alderwick LJ, Futterer K (2013) Synthesis of alpha-glucan in mycobacteria involves a hetero-octameric complex of trehalose synthase TreS and Maltokinase Pep2. ACS Chem Biol **8**:2245-2255

Schuster FL, Visvesvara GS (2004) Free-living amoebae as opportunistic and non-opportunistic pathogens of humans and animals. Int J Parasitol **34**:1001–1027

Tamura K, Stecher G, Peterson D, Filipski A, Kumar S (2013) MEGA6: Molecular evolutionary genetics analysis version 6.0. Mol Biol Evol **30**:2725-2729

Thevelein JM (1984) Regulation of trehalose mobilization in fungi. Microbiol Rev **48**:42-59

Wannet WJB, Op den Camp HJM, Wisselink HW, Van der Grift W, Van Griensven LJLD, Vogels GD (1998) Purification and characterization of trehalose phosphorylase from the commercial mushroom *Agaricus bisporus.* Biochim Biophys Acta (BBA) **1425**:177-188

Watkins RF, Gray MW (2008) Sampling gene diversity across the supergroup Amebozoa: Large EST data sets from *Acanthamoeba castellanii*, *Hartmannella vermiformis*, *Physarum polycephalum*, *Heperamoeba dachnaya* and *Hyperamoeba* sp. Protist **159**:269-281

Weisman RA (1976) Differentiation in *Acanthamoeba castellanii*. Annu Rev Microbiol **30**:189–219

Yu Y, Zhang H, Zhu G (2010) Plant-type trehalose synthetic pathway in *Cryptosporidium* and some other apicomplexans. PLoS ONE **5**:e12593

Figure Legends

Figure 1. Phylogenetic position of the putative trehalose synthase (TreS) from *Acanthamoeba castellanii* within glycoside hydrolases. Consensus tree based on Bayesian, ML and NJ analyses. The label Cterm TreS denotes the group of bacterial enzymes where the TreS domain is fused to a putative kinase C-terminal domain (lacking in amoebae).

Figure 2. Sequence alignment between TreS of *Acanthamoeba castellanii* (TreS_Aca), *Mycobacterium smegmatis* (TreS_sme, GenBank accession ID: YP_006571064) and *M. tuberculosis* (TreS_tuber, GenBank accession ID: EFI32604). Colored boxes highlight the domain organization: domain A (green), domain B (yellow), and domain C (red). Catalytic residues are shown within red boxes.

Figure 3. Phylogenetic position of the TPS-TPP fusion enzymes from *Acanthamoeba castellanii*. A maximum likelihood tree. Three enzymes of this family are present in *A. castellanii*, falling into 2 types: i) primitive proteins placed at the base of all eukaryotic sequences (TPS-TPP 1) and ii) group located at the base of the fungal enzymes (TPS_TPP 2A, B).

Figure 4. Multiple sequence alignment of the TPS domains of the TPS-TPP enzymes (tps-tpp_2a, 2b, tps_tpp_1) from *A. castellanii* and *S. cerevisiae* and the OtsA from *E. coli* (1GZ5). Catalytic residues, based on the analysis of the OtsA structure (Gibson et al. 2002), are highlighted by red boxes. Note that the proteins Tsl1 and Tps3 of *S. cerevisiae* are not enzymatically active.

Figure 5. Multiple sequence alignment of the TPP domains of the TPS-TPP enzymes (tps-tpp_2a, 2b, tps_tpp_1_Aca) from *A. castellanii* and *S. cerevisiae* and the TPP from *T. acidophilum* (1U02). Catalytic residues, based on the analysis of the 1U02 structure (Rao et

al. 2006), are highlighted by red boxes. Note that the proteins Tsl1 and Tps3 of *S. cerevisiae* are not enzymatically active.

Figure 6. Changes in the amounts of mRNA for the trehalose synthetic pathway genes during *Acanthamoeba* pseudocyst formation **(A)** and encystation **(B).** The changes in the amounts of the mRNA transcripts of the four genes of the trehalose synthetic pathways found in the *Acanthamoeba* genome at several time points during encystation and pseudocyst formation compared to the situation at the trophozoite stage (time zero) were measured by qRT-PCR. The gene for *Acanthamoeba* 18S rDNA was used as a reference.

Figure 7. Carbohydrate levels during *Acanthamoeba* pseudocyst formation **(A)** and encystation **(B).** The carbohydrates were isolated from 1×10^7 *Acanthamoeba* cells and quantified using external calibration HILIC ESI-qTOF-MS. The carbohydrate levels at time point 0.1 hour are the initial amount present in the trophozoite stage before differentiation initiation. The left Y-axis corresponds to trehalose and maltose, right Y-axis is for glucose, axes apply to both panels.

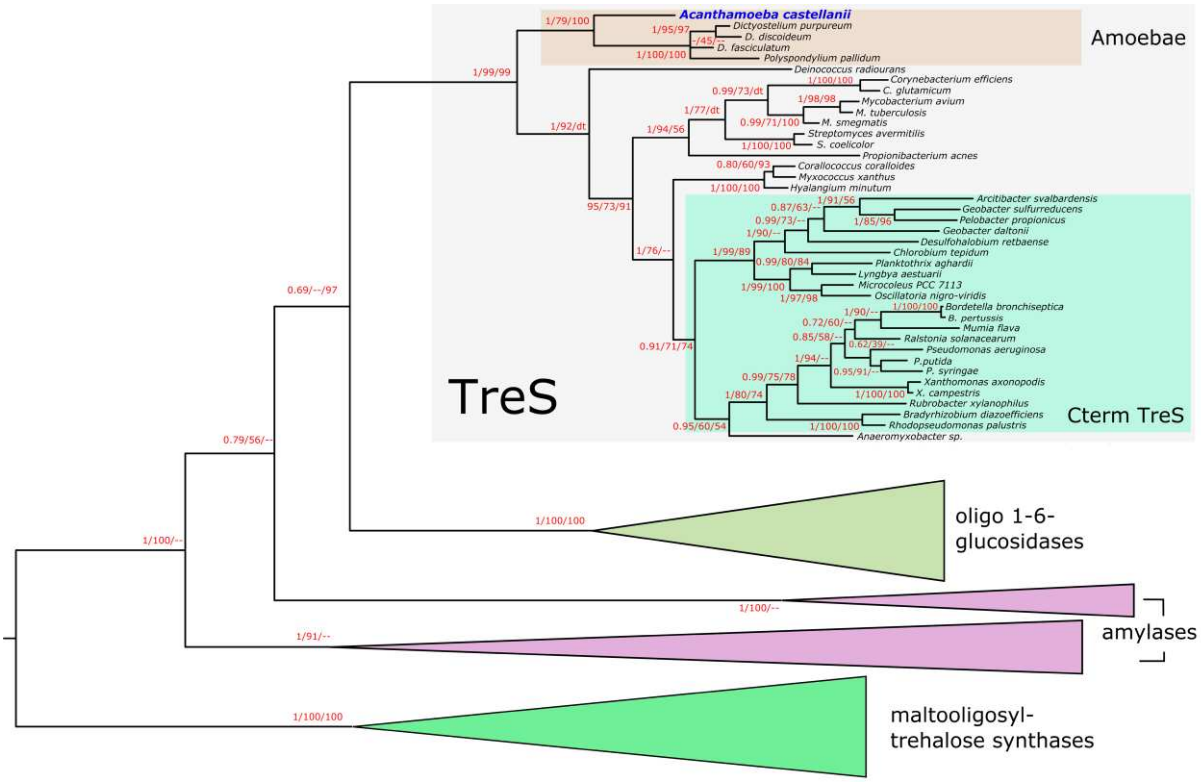

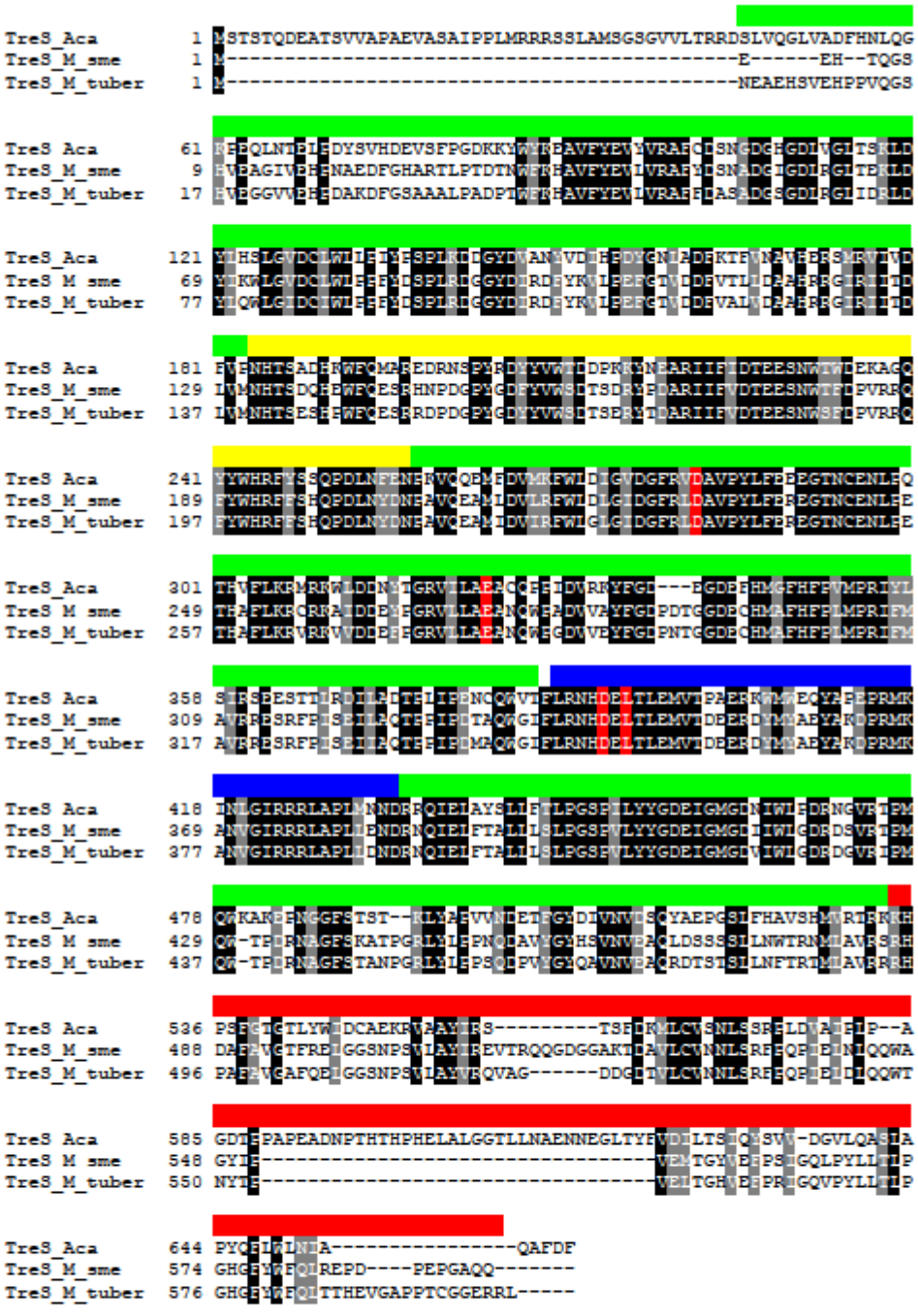

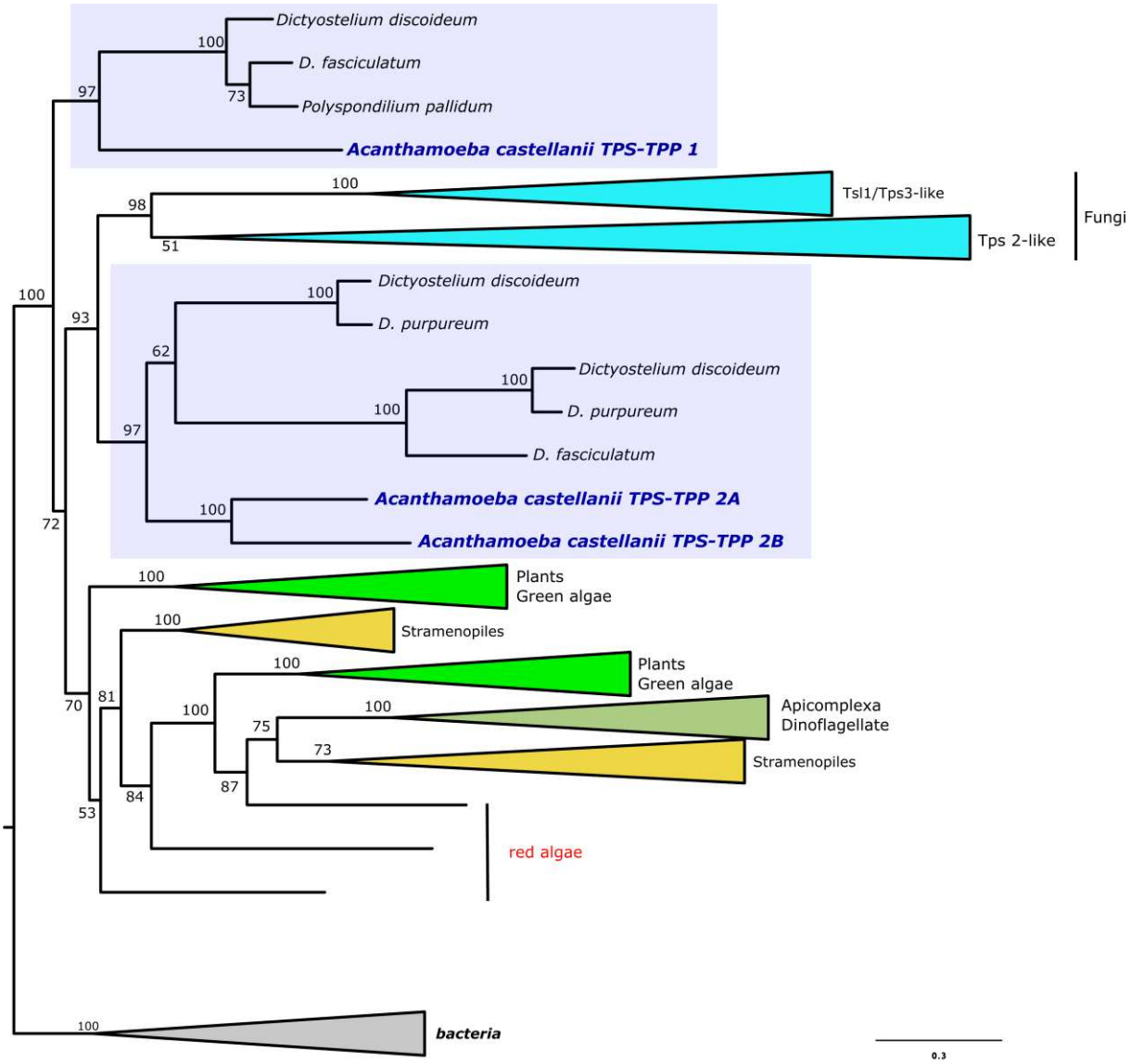

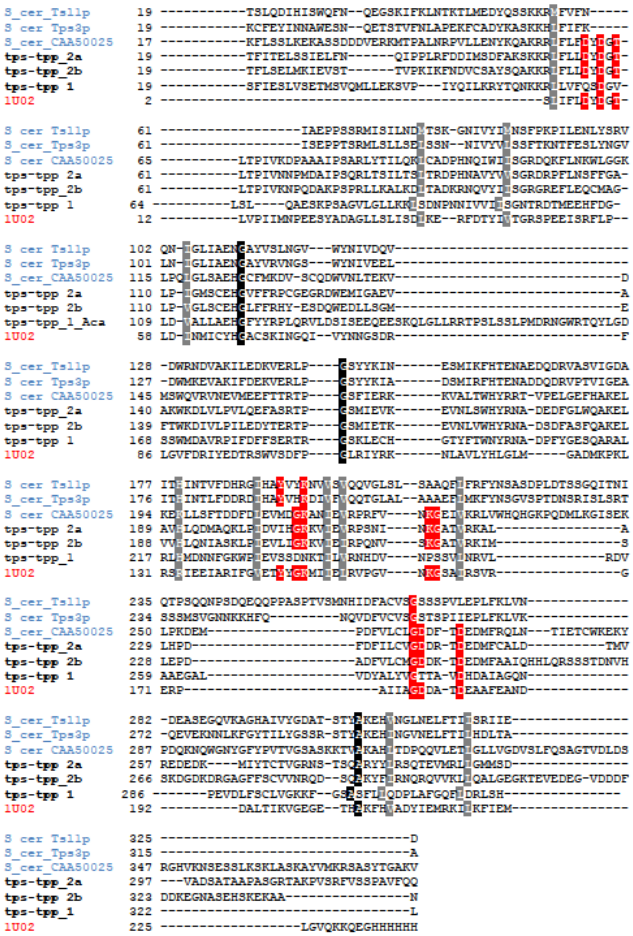

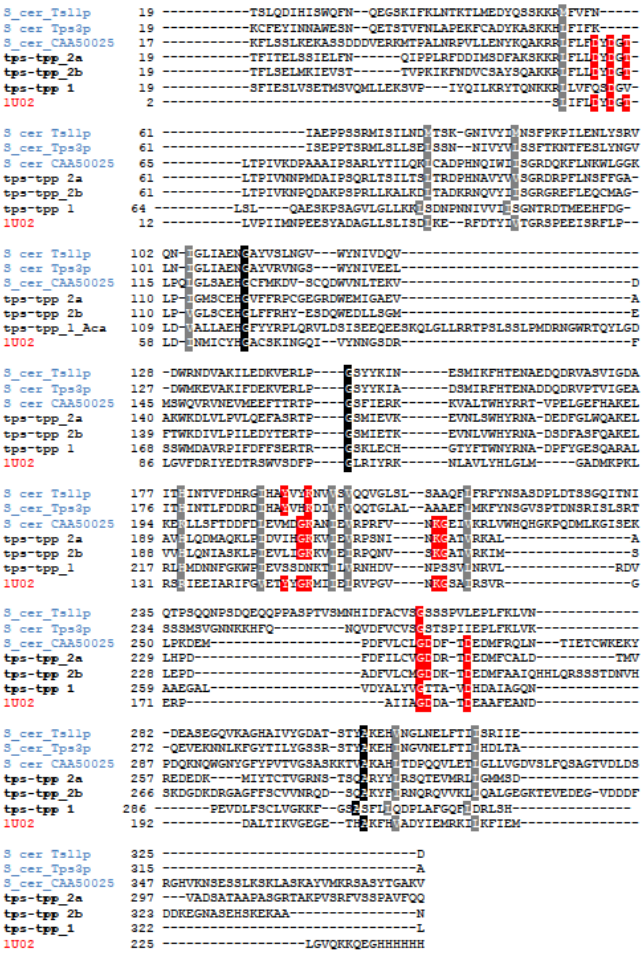

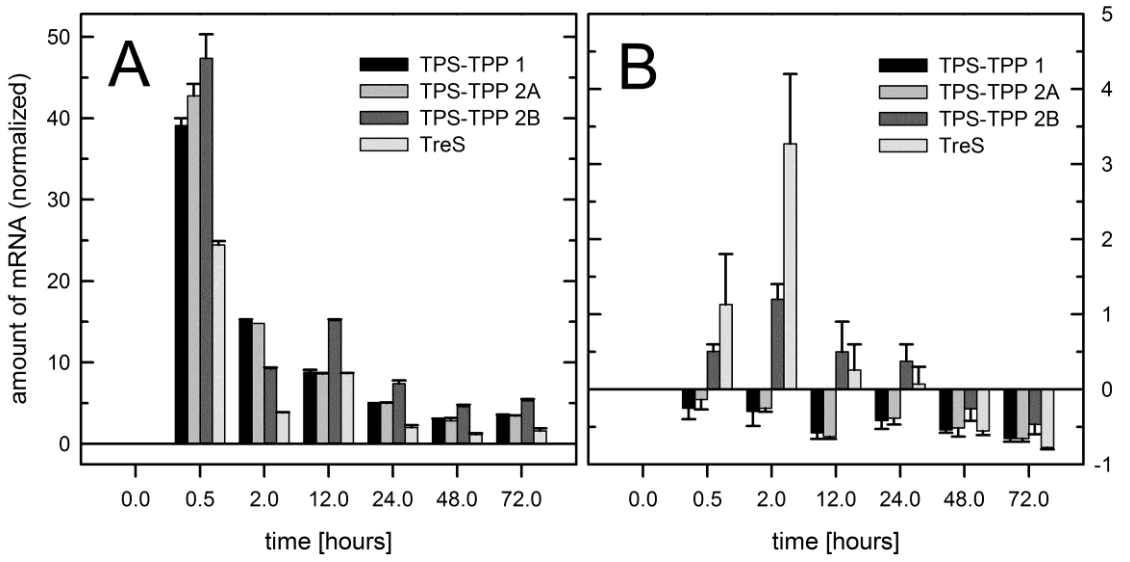

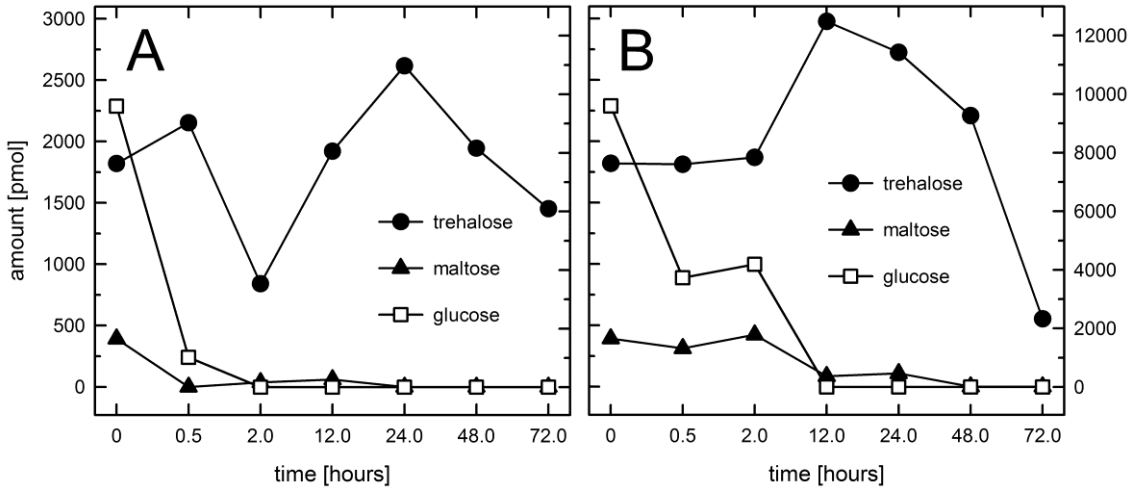

Table 1. Gene-specific forward and reverse primers used for qRT-PCR amplification

gene	Forward primer sequence (5´ - 3´)	Reverse primer sequence (5´ - 3´)
TPS-TPP 1	TCA AGA CCC TCC CTG AAA	ACG GGC AGA ATA CGA TAG A
TPS-TPP 2A	TCA AGA CCC TCC CTG AAA	ACG GGC AGA ATA CGA TAG A
TPS-TPP 2B	CCC GAT TTC GAC TTC ATC TT	ATC ATC TTG TCC TCG TCC T
TreS	GGC CCG CAT CAT CTT TAT C	CCT TGG GAT TCT CGA AGT TAA G
18S rDNA	TGC ATG GCC GTT CTT AGT TGG	AGC GCG GCA TAT TTA GCA GGT